Journal of Medicinal Chemistry

Brief Article

pubs.acs.org/jmc

De Novo Fragment Design: A Medicinal Chemistry Approach to Fragment-Based Lead Generation

Francisco X. Talamas,* Gloria Ao-Ieong, Ken A. Brameld, Elbert Chin, Javier de Vicente, James P. Dunn, Manjiri Ghate, Anthony M. Giannetti, Seth F. Harris, Sharada S. Labadie, Vincent Leveque, Jim Li, Alfred S-T. Lui, Kristen L. McCaleb, Isabel Nájera, Ryan C. Schoenfeld, Beihan Wang, and April Wong

Hoffmann-La Roche Inc., Pharma Research & Early Development, 340 Kingsland Street, Nutley, New Jersey 07110, United States

Supporting Information

ABSTRACT: The use of fragments with low binding affinity for their targets as starting points has received much attention recently. Screening of fragment libraries has been the most common method to find attractive starting points. Herein, we describe a unique, alternative approach to generating fragment leads. A binding model was developed and a set of guidelines were then selected to use this model to design fragments, enabling our discovery of a novel fragment with high LE.

INTRODUCTION

In the last two decades, fragment screening has been embraced by the pharmaceutical and biotechnology industry, becoming an integral part of drug discovery. Much of this can be attributed to the early success of several companies that developed fragments into clinical candidates[1,2] or a marketed drug.[3]

Fragments as starting points for lead identification efforts are typically found by using two complementary approaches: (1) screening a library of fragments or (2) by de novo fragment design using computer-assisted methods. The use of fragment libraries is the most common approach. A summary of the process and successes of using libraries for fragment-based drug discovery has been documented by Erlanson.[4] Two decades ago, computer-assisted de novo design methods such as LEGEND[5] attracted the attention of researchers to use computational tools to create novel structures that could become drugs. Since then, a large number of new programs have been described in the literature that addresses the approach of de novo design. Two excellent reviews by Loving[6] and Rognan[7] describe the methods and approaches used by the different programs. Even with the success obtained by using software to do de novo fragment design, some drawbacks have been identified and are difficult to overcome.[7]

Herein, we describe our approach to de novo fragment design targeting the hepatitis C virus (HCV) nonstructural 5B (NS5B) polymerase that plays an important role in the life cycle of the virus by replicating the viral genome.[8] We approached de novo fragment design by implementing some of the same principles utilized by computer programs. Key receptor interactions were identified, and design constraints were defined. The generation of the novel compounds was done differently. The fragments were created by medicinal chemists that applied their own experience to design novel molecules that addressed all the recognized disadvantages.

RESULTS AND DISCUSSION

A library of ~2700 fragments was screened against the HCV NS5B polymerase using surface plasmon resonance (SPR) and confirmed 163 hits. Using different parameters, 29 fragments were selected for crystallography but only fragment **1** cocrystallized with NS5B (NS5B BK K_D = 78 μM and IC_{50} = 130 μM). Attempts to directly improve potency, and some of the physicochemical and ADME properties of the scaffold provided by **1** were unsuccessful.

At the same time that the screening activities were ongoing, a de novo fragment design approach was also taken to come up with leads that could then be moved into optimization as an alternative to library screening. Of the four allosteric sites in NS5B known,[9] the palm I site was selected for targeting using this approach.

Our first step was to build a model containing key interactions in the palm I allosteric site. We used the crystallographic data available from our internal efforts (**2** and **3**[10,11]) and the relevant structures in the public domain (**4**–**6**[12−14]) available at the time (early 2007).

As mentioned above, we were not able to use **1** as an explicit starting point for our medicinal chemistry efforts, however, **1** played an important role in helping us develop our model. Careful analysis of the crystallographic data revealed that the pyrazolopyrimidine N-2 makes a hydrogen bond accepting interaction with the backbone NH of Tyr448, and the NH hydrogen on the N-1 was within hydrogen bond distance (2.4 Å) to the backbone carbonyl of Gln446 (Figure 1). This interaction with Gln446 was unexpected and to our knowledge the first time that a small molecule binding in the palm I site exhibited it.

Once we had selected the relevant molecules (**1**–**6**) from which to develop the model, it was decided to focus mainly on the hydrophobic area of the allosteric site (for additional descriptions of all the interactions in this site see ref 10). First,

Received: February 19, 2013

   dx.doi.org/10.1021/jm4002605 | J. Med. Chem. XXXX, XXX, XXX−XXX

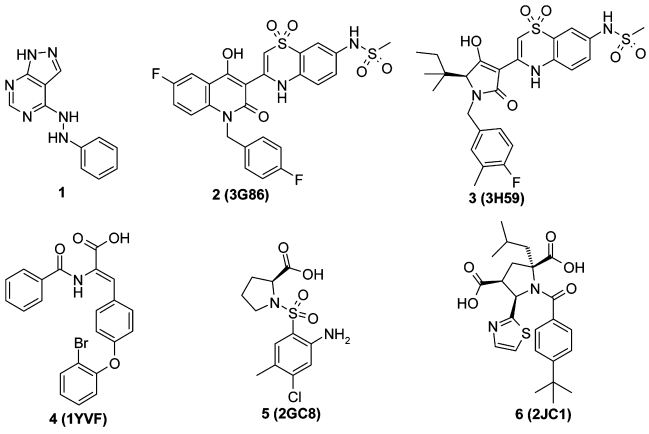

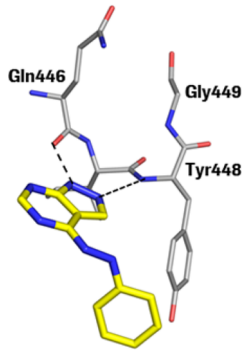

Figure 1. Co-crystal structure of fragment **1** with HCV NS5B polymerase. Simplified view of the binding of **1** in the palm I allosteric site. Dashed lines indicate the hydrogen bond interactions of the ligand with the backbone residues.

it was recognized that all the inhibitors made a primary interaction not only with the backbone NH of Tyr448 but also with either the carbonyl of Gln446, as described for **1**, or with the NH of Gly449 through a conserved molecule of water (**2** and **3**) or directly (**5** and **6**). It was also observed that the hydrophobic pocket can expand and has a relatively wide entry point that accommodates hydrophobic groups of different sizes from different directions. The largest pocket observed was with **4**. The importance of the aryl side chain of Tyr448 was also recognized, as all of **1**–**6** make aromatic edge-to-face interactions. Hydrophobic interactions with Gly410 and/or Met414 side chain were observed with all the inhibitors. An idealized design model was constructed utilizing all of these important interactions for the purpose of de novo design (Figure 2).

With the model in place, the following set of guidelines were proposed for the design of de novo fragments: (a) satisfy backbone carbonyl of Gln446 and NH of Tyr448, optionally displacing or engaging the conserved molecule of water, (b) occupy large hydrophobic pocket, probing with variable groups to satisfy pocket size, (c) position an aromatic group to make edge-to-face interaction with the aryl side chain group of Tyr448, and (d) include at least one hydrophobic interaction with Gly410 and/or Met414. The following steps were followed for the design and selection of targets: the medicinal chemist discussed his ideas with the computational chemist and modeled them. In a routine manner, the ideas were discussed and brainstormed within the team and collectively selected the most promising proposals for synthesis.

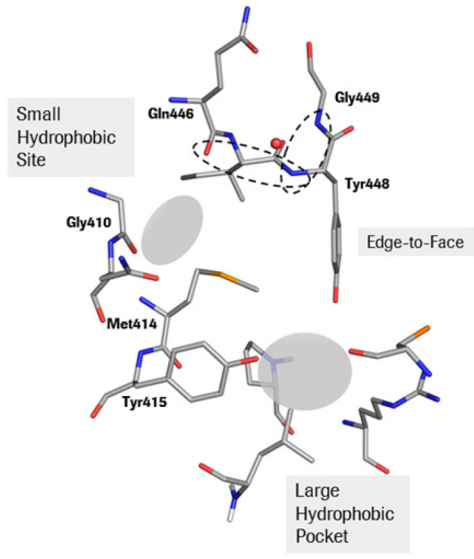

Figure 2. Model depicting key interactions. Displayed are the identified amino acids important for the binding of the known inhibitors. The dashed circles indicate possible modes of hydrogen bond donor–acceptor interactions with the backbone, and the gray areas represent volumes where hydrophobic interactions were identified. The red sphere represents a conserved molecule of water.

It was preferred at this point of the program to focus on molecules with no acidic functionality to avoid potential issues with permeability. Because fragment **1** was the only known binder to palm I without an acidic moiety, we focused on incorporating the unique NH Gln446 interaction into our design. The first step was to identify ring systems containing a hydrogen donor (NH) and an acceptor (N or O) separated by two, three, or four bonds.

A comprehensive set of heterocycles satisfying these criteria was derived from the CSD and a ring system identification algorithm.[15] All docking, energy minimization, and visual analyses were performed using the Molecular Operating Environment (MOE).[16] The initial pose in the binding pocket of each heterocycle was generated using a three-point pharmacophore defining the ideal location of the hydrogen bond donor, hydrogen bond acceptor, and a ring center, each with a radius of 1 Å. These initial poses were then subjected to energy minimization with the MMFF94s forcefield using the "R-field" solvent model. The RMSD of the pharmacophore points for the energy minimized coordinates was used to rank order the heterocycles for visual analysis. Each heterocycle was visually studied both for the ability to satisfy the desired hydrogen bonds and to provide a vector toward the other key interaction points. In general, the ring systems capable of 1,2- and 1,3-interactions modeled the best, some of them shown in Figure 3.

Ligand efficiency[17] (LE) was tracked during this process to drive the design toward efficient binders because it has been shown that the initial LE for a lead is maintained or decreases as the series evolve to a clinical candidate.[18]

This process can be exemplified with the imidazol-2-one moiety (Figure 4). When this ring system was modeled, it was apparent that good interactions with the backbone carbonyl Gln446 and NH Tyr448 could be made. One of the ring nitrogens was in a position to grow toward the hydrophobic pocket (yellow arrow). When this model was overlapped with **1** (in gray), this assumption was confirmed and it was also noted

dx.doi.org/10.1021/jm4002605 | J. Med. Chem. XXXX, XXX, XXX–XXX

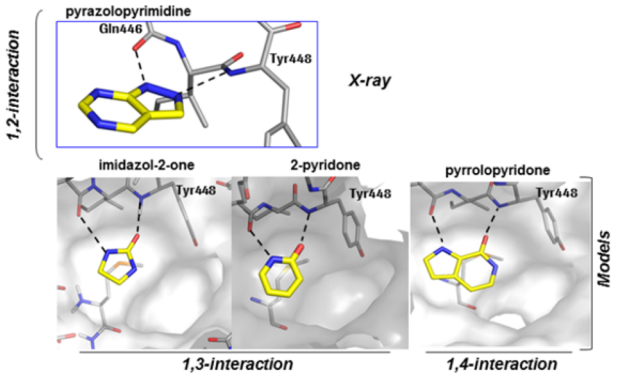

Figure 3. Ring systems with hydrogen bond donor−acceptor functionalities modeled in the hydrophobic area of palm I site.

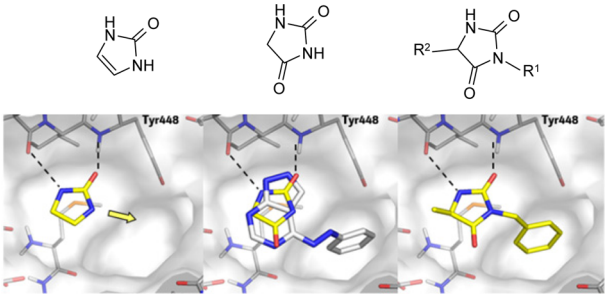

Figure 4. Evolution of imidazol-2-one to a disubstituted hydantoin.

that N-5 nitrogen on the pyrimidine portion of **1** could be mimicked by adding a carbonyl group to the five-membered ring system, changing the imidazol-2-one to a hydantoin ring system. In turn, the hydantoin could give us the opportunity to add alkyl groups (R^2) on C-5 to interact with Gly410 (small hydrophobic site).

First, fragment **7** was prepared and screened but did not show any measurable activity in the biochemical assay (Table 1). Adding 3,4-dichloro substitution to the aryl ring (**8**) did not show any improvement, but 4-*t*-butyl substitution (**9**) started showing some activity. Other substitutions on the aryl ring did not improve the activity of this early fragment. After having fulfilled three of the requirements in our model (carbonyl Gln446/NH Tyr448 backbone interactions, filling of hydrophobic pocket and edge-to-face with Tyr448), we explored the R^3 substitution on the hydantoin to make interactions with the hydrophobic site. Interacting with this part of the palm I site proved to be important to gain extra affinity. As seen in Table 1, as the size of the alkyl group (R^3) increased from hydrogen (**9**, IC_{50} = 364 μM) to *i*-propyl (**12**, IC_{50} = 21 μM), the potency improved by more than 15-fold. Fragment **12** was cocrystallized with NS5B and confirmed the expected binding mode as described above (Figure 5). Up to this point, our model and guidelines had helped us design a novel fragment for the NS5B polymerase.

Another ring system that showed good interactions when modeled into the hydrophobic pocket of the palm I site was the 2-pyridone moiety (Figure 3). The NH and carbonyl of the pyridone looked to be able to provide good hydrogen bond distances to the two relevant interactions on the backbone. Analyzing the positions to grow toward the lipophilic pocket, C-3 of the pyridone appeared to be a reasonable choice to add substitutions. The pyridone with the 4-*t*-benzyl group (**13**) on

Table 1. Evolution of Hydantoin and Pyridone Fragments[a]

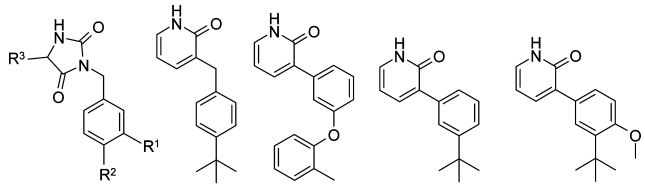

7-12 13 14 15 16

compd	R^1	R^2	R^3	IC_{50} (μM)	K_D (μM)	LE
1				130	78	0.31
7	H	H	H	>1000	NA	
8	Cl	Cl	H	>1000	NA	
9	H	*t*-butyl	H	364	400	0.26
10	H	*t*-butyl	methyl	220	144	0.26
11	H	*t*-butyl	ethyl	108	93	0.27
12	H	*t*-butyl	*i*-propyl	21	18	0.30
13				431	NA	0.26
14				80	NA	0.27
15				4.0	5.8	0.43
16				0.44	0.57	0.46

[a] IC_{50} were measured using GT-1b NS5B Con1 strain (**7**−**16**) and GT-1b NS5B BK strain (**1**). K_D was measured using GT-1b NS5B BK strain. IC_{50} and K_D values are the average of at least two experiments. LE is calculated using the IC_{50} value in the formula reported by Groom[17].

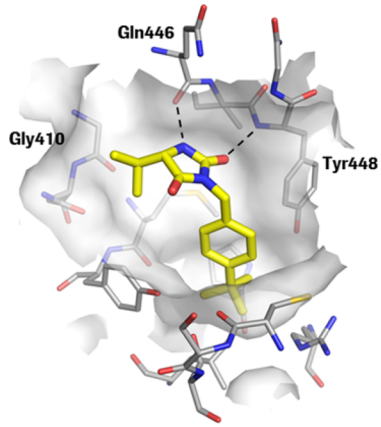

Figure 5. Co-crystal structure of fragment **12** with HCV NS5B polymerase in palm I allosteric site.

C-3 was synthesized and screened in the enzyme assay against NS5B, displaying similar activity as **9** (Table 1).

Another way to fill the lower pocket, based on modeling, was by directly attaching on the C-3 position of the pyridone an aryl ring with a substituent on the meta position. We started with one of the groups initially reported by Pfizer.[12] Fragment **14** was prepared and presented an increase in potency with respect to the previous fragment, however, the ligand efficiency stayed the same. The use of LE at this point of fragment design was very useful because it was an excellent metric to indicate if the changes improved the binding affinity of our fragments. Because of the null gain in LE by attempting to fill the large hydrophobic pocket, we explored again the use of the *t*-butyl group. Fragment **15**, with a *t*-butyl group in the meta position, was prepared and screened in the enzyme assay to give an IC_{50} = 4.0 μM, over 100-fold increase in potency with respect to **13**.

The properties of **15** stayed within the desired range (calculated pK_a 10.4 and PSA 26) and had an excellent LE of

dx.doi.org/10.1021/jm4002605 | J. Med. Chem. XXXX, XXX, XXX−XXX

0.43. Co-crystallization of **15** with NS5B confirmed that the fragment was binding in the palm I site (Figure 6) as expected.

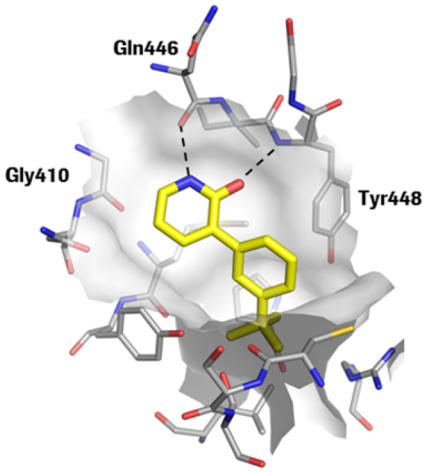

Figure 6. Co-crystal structure of fragments **15** with HCV NS5B polymerase in palm I allosteric site. A figure overlaying the cocrystal structures of the protein bound to fragment **1** and fragment **15** can be found in the Supporting Information.

It is important to notice that the de novo designed fragment **15** exhibits significantly more potent enzymatic activity and binding affinity than **1**, found in our library, while both have the same number of heavy atoms (17) and thus **15** has a much higher LE than **1** (0.43 vs 0.31).

Introduction of the methoxy group on the 4-position of the aryl ring of **15** gave a 10-fold increase in potency and improved the LE to 0.46 (fragment **16**). A similar effect was observed by the GSK group on their template.[14] Fragment **16** was further optimized to become a clinical candidate that entered phase I. The clinical candidate, which has a LE of 0.35, contains all the atoms present in this fragment.

Figures were drawn with PyMOL.[19]

CONCLUSION

In this paper, we described a novel approach for de novo fragment design that relies on the design by medicinal chemists. The approach allowed us to incorporate all the relevant characteristics during the design of the fragments (synthetic route, uniqueness of the fragments with respect to prior art, and drug-like properties) to minimize the efforts and time to find an excellent starting point for the program. This is the first case, to our knowledge, in which medicinal and computational chemists applied structure-based methodologies to the de novo design of a complete fragment by following a predefined set of interaction criteria.

This approach offers several advantages compared to virtual screening or de novo fragment design using only computational methods. We believe that the unique process described in this paper can also be successfully applied to other targets for which it may be difficult to otherwise find high quality starting leads.

ASSOCIATED CONTENT

Supporting Information

Experimental procedure for the preparation of **7**−**16**, spectroscopic data of intermediates and target compounds, description of the HCV NS5B polymerase biochemical and surface plasma resonance assays, and crystallographic protocols and information for cocrystals of NS5B with **1**, **12**, and **15**. This material is available free of charge via the Internet at http://pubs.acs.org.

Accession Codes

The coordinates and structure factor files have been deposited in the Protein Data Bank under the accession codes 4IH5 (**1**), 4IH6 (**12**), and 4IH7 (**15**).

AUTHOR INFORMATION

Corresponding Author

*Phone: (973) 235-3626. E-mail: franciscotalamas@gmail.com.

Notes

The authors declare no competing financial interest.

ACKNOWLEDGMENTS

We gratefully acknowledge all members of the Analytical Department in Roche Palo Alto and the Physical Chemistry Department at Hoffmann-La Roche, Nutley, for the characterization of the compounds. We thank Romyr Dominique for helpful discussions. The Advanced Light Source is supported by the Director, Office of Science, Office of Basic Energy Sciences, of the U.S. Department of Energy under contract no. DE-AC02-05CH11231.

ABBREVIATIONS USED

HCV, hepatitis C virus; NS5B, nonstructural 5B

REFERENCES

(1) Wendt, M. D. Discovery of ABT-263, a Bcl-Family Protein Inhibitor: Observations on Targeting a Large Protein−Protein Interaction. *Expert Opin. Drug Discovery* **2008**, *3*, 1123−1143.

(2) Wyatt, P. G.; Woodhead, A. J.; Berdini, V.; Boulstridge, J. A.; Carr, M. G.; Cross, D. M.; Davis, D. J.; Devine, L. A.; Early, T. R.; Feltell, R. E.; Lewis, E. J.; McMenamin, R. L.; Navarro, E. F.; O'Brien, M. A.; O'Reilly, M.; Reule, M.; Saxty, G.; Seavers, L. C. A.; Smith, D. M.; Squires, M. S.; Trewartha, G.; Walker, M. T.; Woolford, A. J. A. Identification of *N*-(4-Piperidinyl)-4-(2,6-dichlorobenzoylamino)-1*H*-pyrazole-3-carboxamide (AT7519), A Novel Cyclin Dependent Kinase Inhibitor Using Fragment-Based X-Ray Crystallography and Structure Based Drug Design. *J. Med. Chem.* **2008**, *51*, 4986−4999.

(3) Bollag, G.; Tsai, J.; Zhang, J.; Zhang, Ch.; Ibrahim, P.; Nolop, K.; Hirth, P. Vemurafenib: The First Drug Approved for BRAF-Mutant Cancer. *Nature Rev. Drug Discovery* **2012**, *11*, 873−886.

(4) Erlanson, D. A. Introduction to Fragment-Based Drug Discovery. *Top. Curr. Chem.* **2012**, *317*, 1−32.

(5) Nishibata, Y.; Itai, A. Automatic Creation of Drug Candidate Structures Based on Receptor Structure. Starting Point for Artificial Lead Generation. *Tetrahedron* **1991**, *47*, 8985−8990.

(6) Loving, K.; Alberts, I.; Sherman, W. Computational Approaches for Fragment-Based and de Novo Design. *Curr. Top. Med. Chem.* **2010**, *10*, 14−32.

(7) Rognan, D. Fragment-Based Approaches and Computer-Aided Drug Discovery. *Top. Curr. Chem.* **2012**, *317*, 201−222.

(8) Sofia, M. J.; Chang, W.; Furman, P. A.; Mosley, R. T.; Ross, B. S. Nucleoside, Nucleotide, and Non-Nucleoside Inhibitors of Hepatitis C Virus NS5B RNA-Dependent RNA-Polymerase. *J. Med. Chem.* **2012**, *55*, 2481−2531.

(9) Le Pogam, S.; Seshaadri, A.; Kosaka, A.; Chiu, S.; Kang, H.-S.; Hu, S.; Rajyaguru, S.; Symons, J.; Cammack, N.; Najera, I. Existence of Hepatitis C Virus NS5B Variants Naturally Resistant to Non-Nucleoside, but not to Nucleoside, Polymerase Inhibitors Among Untreated Patients. *J. Antimicrob. Chemother.* **2008**, *61*, 1205−1216.

(10) de Vicente, J.; Hendricks, R. T.; Smith, D. B.; Fell, J. B.; Fischer, J.; Spencer, S. R.; Stengel, P. J.; Mohr, P.; Robinson, J. E.; Blake, J. F.; Hilgenkamp, R. K.; Yee, C.; Adjabeng, G.; Elworthy, T. R.; Tracy, J.;

Chin, E.; Li, J.; Wang, B.; Bamberg, J. T.; Stephenson, R.; Oshiro, C.; Harris, S. F.; Ghate, M.; Leveque, V.; Najera, I.; Le Pogam, S.; Rajyaguru, S.; Ao-Ieong, G.; Alexandrova, L.; Larrabee, S.; Brandl, M.; Briggs, A.; Sukhtankar, S.; Farrell, R.; Xu, B. Non-Nucleoside Inhibitors of HCV Polymerase NS5B. Part 2: Synthesis and Structure−Activity Relationships of Benzothiazine-Substituted Quinolinediones. *Bioorg. Med. Chem. Lett.* **2009**, *19*, 3642−3646.

(11) de Vicente, J.; Hendricks, R. T.; Smith, D. B.; Fell, J. B.; Fischer, J.; Spencer, S. R.; Stengel, P. J.; Mohr, P.; Robinson, J. E.; Blake, J. F.; Hilgenkamp, R. K.; Yee, C.; Zhao, J.; Elworthy, T. R.; Tracy, J.; Chin, E.; Li, J.; Lui, A.; Wang, B.; Oshiro, C.; Harris, S. F.; Ghate, M.; Leveque, V. J. P.; Najera, I.; Le Pogam, S.; Rajyaguru, S.; Ao-Ieong, G.; Alexandrova, L.; Fitch, B.; Brandl, M.; Masjedizadeh, M.; Wu, S.; de Keczer, S.; Voronin, T. Non-Nucleoside Inhibitors of HCV Polymerase NS5B. Part 3: Synthesis and Optimization Studies of Benzothiazine-Substituted Tetramic Acids. *Bioorg. Med. Chem. Lett.* **2009**, *19*, 5648−5651.

(12) Pfefferkorn, J. A.; Greene, M. L.; Nugent, R. A.; Gross, R. J.; Mitchell, M. A.; Finzel, B. C.; Harris, M. S.; Wells, P. A.; Shelly, J. A.; Anstadt, R. A.; Kilkuskie, R. E.; Koptab, L. A.; Schwendea, F. J. Inhibitors of HCV NS5B Polymerase. Part 1: Evaluation of the Southern Region of (2*Z*)-2-(Benzoylamino)-3-(5-phenyl-2-furyl)-acrylic Acid. *Bioorg. Med. Chem. Lett.* **2005**, *15*, 2481−2486.

(13) Gopalsamy, A.; Chopra, R.; Lim, K.; Ciszewski, G.; Shi, M.; Curran, K. J.; Sukits, S. F.; Svenson, K.; Bard, J.; Ellingboe, J. W.; Agarwal, A.; Krishnamurthy, G.; Howe, A. Y. M.; Orlowski, M.; Feld, B.; O′Connell, J.; Mansour, T. S. Discovery of Proline Sulfonamides as Potent and Selective Hepatitis C Virus NS5b Polymerase Inhibitors. Evidence for a New NS5b Polymerase Binding Site. *J. Med. Chem.* **2006**, *49*, 3052−3055.

(14) Slater, M. J.; Amphlett, E. M.; Andrews, D. M.; Bravi, G.; Burton, G.; Cheasty, A. G.; Corfield, J. A.; Ellis, M. R.; Fenwick, R. H.; Fernandes, S.; Guidetti, R.; Haigh, D.; Hartley, C. D.; Howes, P. D.; Jackson, D. L.; Jarvest, R. L.; Lovegrove, V. L. H.; Medhurst, K. J.; Parry, N. P.; Price, H.; Shah, P.; Singh, O. M. P.; Stocker, R.; Thommes, P.; Wilkinson, C.; Wonacott, A. Optimization of Novel Acyl Pyrrolidine Inhibitors of Hepatitis C Virus RNA-Dependent RNA Polymerase Leading to a Development Candidate. *J. Med. Chem.* **2007**, *50*, 897−900.

(15) Brameld, K. A.; Kuhn, B.; Reuter, D. C.; Stahl, M. Small Molecule Conformational Preferences Derived from Crystal Structure Data. A Medicinal Chemistry Focused Analysis. *J. Chem. Inf. Model.* **2008**, *48*, 1−24.

(16) *Molecular Operating Environment (MOE)*; Chemical Computing Group Inc.: 1010 Sherbooke Street West, Suite #910, Montreal, QC, Canada, H3A 2R7, 2008.

(17) Hopkins, A. L.; Groom, C. R.; Alex, A. Ligand Efficiency: A Useful Metric for Lead Selection. *Drug Discovery Today* **2004**, *9*, 430−431.

(18) Hajduk, P. J. Fragment-Based Drug Design: How Big is Too Big? *J. Med. Chem.* **2006**, *49*, 6972−6976.

(19) *The PyMOL Molecular Graphics System*, version 1.5.0.4; Schrödinger, LLC.